ACS Catalysis

Article

La[N(SiMe3)2]3 – Catalyzed Ester Reductions with Pinacolborane. Scope and Mechanism of Ester Cleavage

Christopher Jeffrey Barger, Alessandro Motta, Victoria L. Weidner, Tracy Lynn Lohr, and Tobin J. Marks

ACS Catal., **Just Accepted Manuscript** • DOI: 10.1021/acscatal.9b02605 • Publication Date (Web): 21 Aug 2019

is published by the American Chemical Society. 1155 Sixteenth Street N.W., Washington, DC 20036

$La[N(SiMe_3)_2]_3$ – Catalyzed Ester Reductions with Pinacolborane. Scope and Mechanism of Ester Cleavage

Christopher J. Barger, Alessandro Motta,[†] Victoria L. Weidner, Tracy L. Lohr,[‡] and Tobin J. Marks**

Department of Chemistry, Northwestern University, 2145 Sheridan Rd, Evanston, Illinois 60208-3113, United States

[†]Dipartimento di Scienze Chimiche, Università di Roma "La Sapienza" and INSTM, UdR Roma, Piazzale Aldo Moro 5, I-00185 Roma, Italy

Lanthanides, homogeneous catalysis, hydroboration, ester reduction, C-O bond cleavage

Abstract. Tris[N,N-bis(trimethylsilyl)amido]lanthanum (La^{NTMS}) is an efficient, highly active, and selective homogeneous catalyst for ester reduction with pinacolborane (HBpin). Alkyl and aryl esters are cleaved to the corresponding alkoxy- and aryloxy-boronic esters which can then be straightforwardly hydrolyzed to alcohols. Ester reduction is achieved with 1 mol% catalyst loading at 25-60°C, and most substrates are quantitatively reduced in 1 hour. Nitro, halide, and amino functional groups are well-tolerated, and ester reduction is completely chemoselective over potentially competing intra- or intermolecular alkene or alkyne hydroboration. Kinetic studies, isotopic labeling, and DFT calculations with energetic span analysis argue that ester reduction proceeds through a rate-determining hydride transfer step that is ligand-centered (hydride is transferred directly from bound HBpin to bound ester) and not through a metal hydride-based intermediate that is often observed in organolanthanide catalysis. The active catalyst is proposed

to be a La-hemiacetal, $[(Me_3Si)_2N]_2$La-OCHR(OR)[HBpin], generated *in situ* from La^{NTMS} via hydroboronolysis of a single La-$N(SiMe_3)_2$ bond. These results add to the growing compendium of selective oxygenate transformations that La^{NTMS} is competent to catalyze, further underscoring the value and versatility of homoleptic lanthanide complexes in homogeneous catalytic organic synthesis.

Introduction

The selective reduction of esters is a topic of great interest to both the academic and industrial synthetic chemistry communities.[1] In addition to being an important transformation in the synthesis of fine chemicals and pharmaceuticals,[2] ester linkages are ubiquitous in lignocellulosic biomass and plant-based oils, valuable renewable sources of fuels and chemical feedstocks, and their selective reduction is of great importance.[3] Unlike ketones and aldehydes, esters are generally inert towards mild reductants as typified by $NaBH_4$ and instead require more aggressive reductants such as BH_3 and $LiAlH_4$, reagents which can pose significant handling risks and often suffer from poor selectivity in the presence of other reducible functionalities.[4] Catalytic hydrogenation has been explored extensively as a more atom-efficient and selective route to ester reduction, however the high pressures and temperatures required to achieve satisfactory conversions, typically in excess of 5 bar and 100°C, pose significant safety concerns, and require capital-intensive equipment.[5] The need for safer and more convenient ester reduction methodologies has generated great interest in recent years in catalytic hydrosilylation, leading to a wealth of reports detailing the selective reduction of esters and other carbonyl groups at ambient pressures and moderate temperatures (typically < 100°C).[6] Conversely, reports of efficient, selective ester hydroboration are sparse,[7] a surprising observation considering that silanes and boranes often behave similarly in

other hydrofunctionalization processes,[1a, 6b, 8] and that hydroboration is well-developed in the context of ketone/aldehyde reduction.[7c, 9]

Encouraged by recent results from this laboratory on lanthanide triflate-catalyzed ester C_{alkoxy}-O bond tandem hydrogenolysis processes, we turned our focus to kinetically labile and electrophilic lanthanide complexes with alternative reducing agents to affect C_{acyl}-O bond reduction, specifically hydroboronolysis (Figure 1A).[10] Tris[N,N-bis(trimethylsilyl)amido]lanthanide complexes ($Ln[N(SiMe_3)_2]_3$, abbreviated here as Ln^{NTMS}, Figure 1B) are commercially available for many lanthanides, or they can be readily

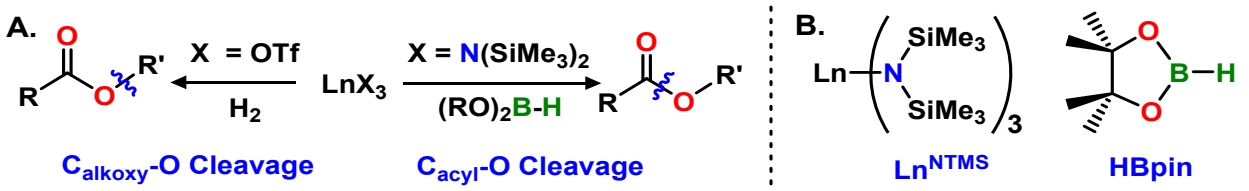

Figure 1. A. Comparison of ester C_{alkoxy}-O bond cleavage/hydrogenolysis, previously reported for lanthanide (Ln) triflates),[10] and Ln-catalyzed C_{acyl}-O bond cleavage/hydroboronolysis pathways (this work). OTf^{-} = $CF_3SO_3^{-}$. **B**. Structures of tris[N,N-bis(trimethylsilyl)amido]lanthanide complexes (Ln^{NTMS}) where Ln = any lanthanide, and pinacolborane (HBpin).

synthesized/purified, rendering them accessible and of great utility to the synthetic methods community.[11] As such, they are frequently employed as precursors to more elaborate lanthanide organometallics[12] and as homogeneous catalysts, particularly for alkene/alkyne hydrofunctionalization.[13] Recently, we reported that La^{NTMS} displays remarkable catalytic activity for ketone and aldehyde hydroboration with HBpin (Figure 1B), with turnover frequencies as high as 40,000 h^{-1} at 25°C.[9l] With this in mind, we sought to explore the catalytic hydroboration activity of La^{NTMS} with more complex, less readily-reduced oxygenates. While this investigation was in progress, Patnaik and Sadow reported that the homoleptic lanthanide tris-hydrocarbyl

$La[C(SiHMe_2)_3]_3$ is highly active for the hydroboration of epoxides and esters, raising the intriguing question of whether commercially available lanthanide amides such as La^{NTMS} might be viable ester hydroboration catalysts, and if so, with what scope and reaction mechanism.[7a]

Here we report that La^{NTMS} effectively mediates the cleavage of a wide variety of alkyl and aryl esters to the corresponding alkoxyboranes. This system, which utilizes a commercially available catalyst, mild reaction conditions, and easily-handled HBpin, represents a significant advance over traditional ester reduction methods. We discuss the scope and mechanism of this transformation through combined experiment and DFT-level theory, which is, to the best of our knowledge, the first attempt to do so in the field of catalytic ester hydroboration. It will be seen that the reaction, which is selective over nitro functionalities as well as alkene and alkyne reductions, proceeds through a La-hemiacetal active catalyst/resting state with a very unusual ligand-centered hydride transfer step.

Results

Ester catalytic reduction scope

Optimal conditions for ester cleavage (Table 1) are achieved with 1 mol % of La^{NTMS} catalyst and a slight excess of HBpin (2.2 equiv vs. ester). Table 1 shows the full scope of esters investigated. Other Ln^{NTMS} complexes (Ln = Ce, Sm, Yb, and Y) were also screened with phenyl benzoate reduction as the model reaction. These catalysts are found to have similar, though slightly diminished reduction rates relative to La^{NTMS}. This, combined with the relative ease with which NMR spectra of metal-organics containing diamagnetic La^{3+} can be analyzed, led us to pursue further studies with La^{NTMS} exclusively. Catecholborane ("HBcat") and 9-borabicyclo[3.3.1]nonane ("9-BBN") were also explored as alternative reductants to HBpin (also using phenyl benzoate reduction as a model reaction). HBcat produces negligible product (<5%)

after 20 hours at 25°C, while 9-BBN affords 46% conversion under the same conditions. These are both significantly poorer performing than HBpin (97% yield after 16 hours at 25°C; Table 1).

As can be seen in Table 1, all esters are reduced near-quantitatively at 25°C under the conditions described above, although several require heating at 60°C for more convenient reaction times (≤ 5 h). Importantly, side-reactions with nitro groups or conjugated alkenes are not observed

Table 1. Scope of La^{NTMS}-catalyzed ester reduction/cleavage with pinacolborane[a]

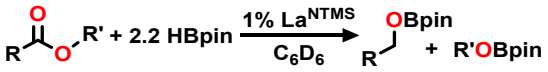

#	Substrate	Product(s)	T/°C	t/h	Yield/%[b]
1	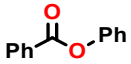	$PhCH_2OBpin$ + PhOBpin	25 60	16 5	97 99
2	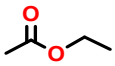	2 EtOBpin	25	0.25	>99
3	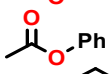	PhOBpin + EtOBpin	25 60	5 1	>99 >99
4	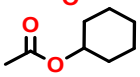	CyOBpin + EtOBpin	25	1	>99
5	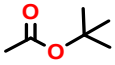	$^tBuOBpin$ + EtOBpin	25 60	16 1	>99 >99
6	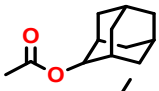	AdmOBpin + EtOBpin	25	1	>99
7[c]	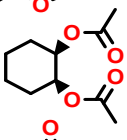	$Cy(OBpin)_2$ + 2EtOBpin	25 60	48 1	98 >99
8	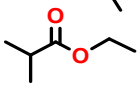	$^iBuOBpin$ + EtOBpin	25	0.25	>99
9	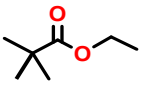	$(CH_3)_3CCH_2OBpin$ + EtOBpin	25	0.5	>99
10	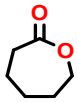	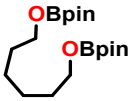	25	0.25	>99
11[d]	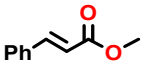	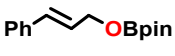	25 60	16 3	>99 >99
12[d]	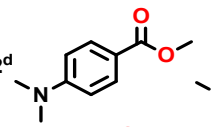	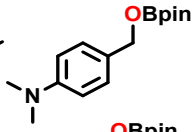	25	16	98
13[d]	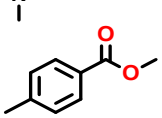	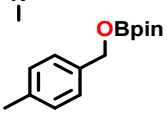	25	1.5	93
14[d]	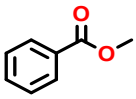	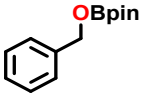	25	1.5	>99
15[d]	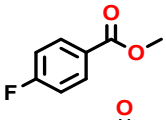	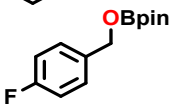	25	1.5	>99
16[d]	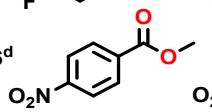	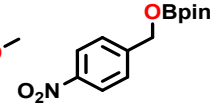	25	0.25	>99

[a] Reaction conditions: Ester (0.25 mmol) and HBpin (0.55 mmol, 2.2 equiv) in C_6D_6 (500 μL), and La^{NTMS} (2.5 μmol). [b] Yields of RCH_2OBpin products calculated by integration of product ^1H NMR signals vs hexamethylbenzene internal standard. [c] 4.4 equiv. HBpin. [d] Product + MeOBpin

(Table 1, entries 16 and 11, respectively), and intermolecular competition experiments indicate that the esters are preferentially reduced with complete exclusion of added 1-octene or 1-octyne (Scheme 1). Given the high activity observed for La^{NTMS}-catalyzed ketone and aldehyde hydroboration,[9l] selectivity for ester reduction over these more reactive functional groups would not be expected. Predictably, reduction of *tert*-butyl acetoacetate occurs only at the ketone, and the ester functionality remains intact, even after 16 hours at 25°C (see SI for details). Preparative-scale (2.5 mmol) reduction of ethyl acetate (entry 2) gives a 94% isolated yield of EtOBpin under conditions identical to those used in the NMR scale reaction.

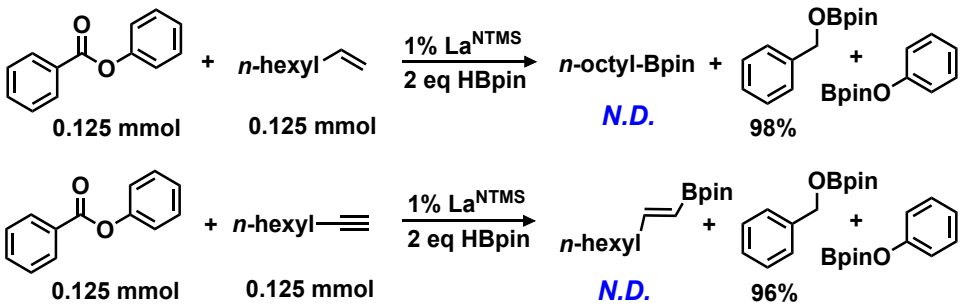

Scheme 1. Competition experiments illustrating the selective reduction of phenyl benzoate in the presence of 1-octene (top) and 1-octyne (bottom). ***N.D.*** = not detected. Conditions: 1.00 mL C_6D_6, 60°C, 5h.

While all ester substrates are efficiently reduced at 60°C, steric impediments at the alkoxy-position (R' in Table 1) significantly depress rates at 25°C, with *tert*-butyl acetate (Table 1, entry 5) requiring 16 h to reach completion, vs. 1 h for cyclohexyl- and 2-adamantyl acetate (entries 4 and 6, respectively) and only 10 min for ethyl acetate (entry 2). Interestingly, steric impediments at the acyl position (R in Table 1) have very little effect on the rate of reduction, with ethyl acetate ethyl isobutyrate, and ethyl pivalate (entries 2, 8, and 9, respectively) all required ≤ 30 min at 25°C to reach completion. The presence of a phenyl group in the R' position (entries 1 and 3) likewise

depresses the rate, suggesting the charge density on the alkoxy oxygen is an important factor in determining the overall conversion rate, possibly implicating La-O coordination in the turnover-limiting step (*vide infra*). Note also that ε-caprolactone (Table 1, entry 10) is reduced quantitatively to the ring-opened bis-borane at 25°C in ~15 min, with no evidence of potentially competing polymerization. This is surprising since the analogous Sm^{NTMS} and Y^{NTMS} complexes are reported to be highly active catalysts for caprolactone ring-opening polymerization.[14] Indeed, when ε-caprolactone is added to a La^{NTMS} solution in benzene without HBpin present, rapid polymerization ensues, as evidenced by solidification of the reaction mixture. Interestingly, subsequent addition of HBpin to the polycaprolactone results in rapid de-polymerization and conversion to a non-viscous liquid that is NMR spectroscopically identical to the product of entry 10 in Table 1.

Experimental kinetic studies

To probe the mechanism of the present ester cleavage process, the rate law for catalytic phenyl benzoate reduction was determined by a combination of initial rates analysis at various catalyst concentrations (for the order in La^{NTMS} concentration) and by monitoring substrate consumption under pseudo-first order conditions (see SI for details). The reaction rate is observed to have a first-order dependence on La^{NTMS} concentration, whereas ester and HBpin concentration variations over a broad range have no detectable effect on the rate (eq. 1). Activation parameters calculated for the reduction of phenyl benzoate over the temperature range of 15-35°C reveal a relatively

$$\text{Rate} = k[La^{NTMS}]^1[\text{Ester}]^0[\text{HBpin}]^0 \quad (1)$$

low apparent activation enthalpy ($\Delta H^{\ddagger} = 8.2 \pm 0.3$ kcal/mol) and a very large, negative activation entropy ($\Delta S^{\ddagger} = -53.1 \pm 0.9$ e.u.). To gauge the impact of electron density at the carbonyl carbon on the rate of reaction, a Hammett plot (Figure 2) was constructed using a series of *para*-substituted

methyl benzoates (Table 1 entries 12-16; see SI for details on rate determination). A significant increase in turnover is observed for substrates with electron-withdrawing substituents at the R position, as indicated by a positive value (1.11) for the parameter ρ. Additional mechanistic details were obtained from isotopic labeling studies. Replacing HBpin with DBpin in the reduction of methyl 4-(*N,N*-dimethylamino)benzoate eliminates both methylene protons in the product ^{1}H NMR spectra, indicating both hydride equivalents are delivered to the carbonyl carbon (Figure 3). Comparing these reaction rates yields a kinetic isotope effect (KIE) of 1.49 (see SI for details).

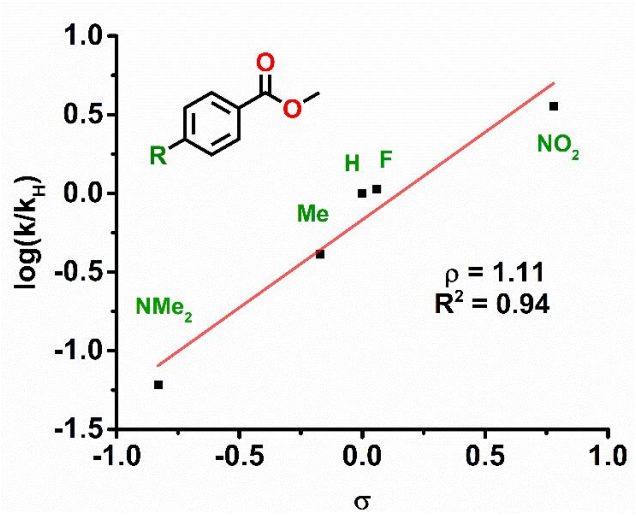

Figure 2. Hammett plot generated for the La^{NTMS}-catalyzed reduction of *para*-substituted methyl benzoates with HBpin.

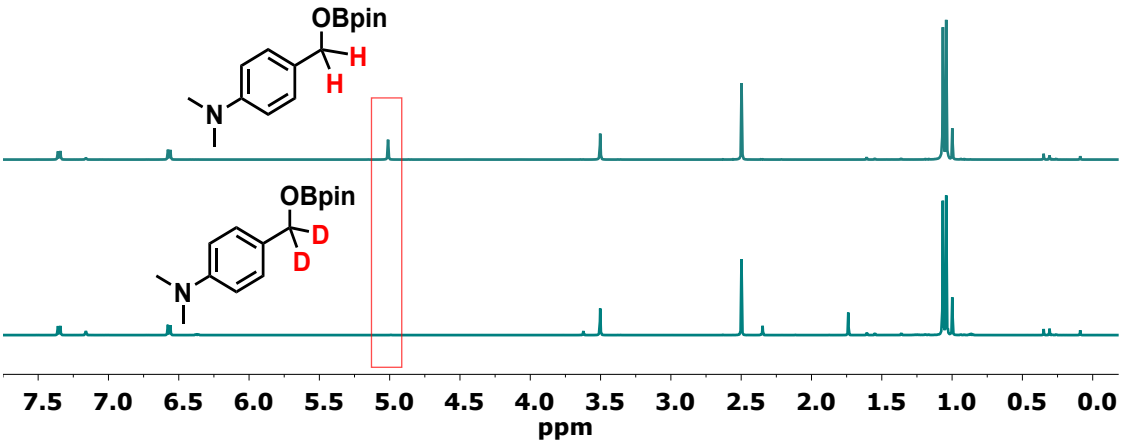

Figure 3. ^{1}H NMR spectra of the La^{NTMS}-catalyzed reduction of methyl 4-(dimethylamino)benzoate with 2 equiv of HBpin (top) and DBpin (bottom). The absence of a signal in the ~δ 5.0 ppm region (outlined in red) for reduction with DBpin shows that both ^{1}H NMR-silent deuteride equivalents are delivered to the carbonyl carbon of the substrate.

In Situ Stoichiometric ^{1}H, ^{13}C and ^{11}B NMR Spectroscopic Studies

The pathway(s) and species involved in the present ester hydroboration process were probed *in situ* by examining the reactivity of La^{NTMS} with stoichiometric amounts of ester and/or HBpin at room temperature. No reaction is observed between La^{NTMS} and phenyl benzoate only, however the ^{1}H NMR signals of both species shift slightly, suggesting that ester reversibly coordinates to Lewis acidic La^{NTMS}.[15] In contrast, La^{NTMS} and HBpin undergo reaction, as evidenced by the appearance of several new signals in the ^{1}H, ^{13}C and, ^{11}B NMR spectra (see SI for spectra and characterization details). In the ^{1}H NMR, singlets at δ 0.37 and 1.03 ppm (integrating as 18 and 12 H, respectively) are attributable to the known compound pinB-N(SiMe$_3$)$_2$.[16] Singlets at δ 1.37 and 1.56 ppm, both integrating to 6 H, as well as a quartet in the ^{11}B NMR at -6.3 ppm, are indicative of a reaction pathway involving ring-opening of a pinacolborane ring to give the off-cycle borate complex shown below (A$_{OC}$, Scheme 2A). A similar complex was reported, by this laboratory, to be an off-cycle product of lanthanocene-catalyzed pyridine dearomatization with pinacolborane (Scheme 2B) and characterized by x-ray diffraction.[17] Notably, in the present system, the La-O bond integrity is

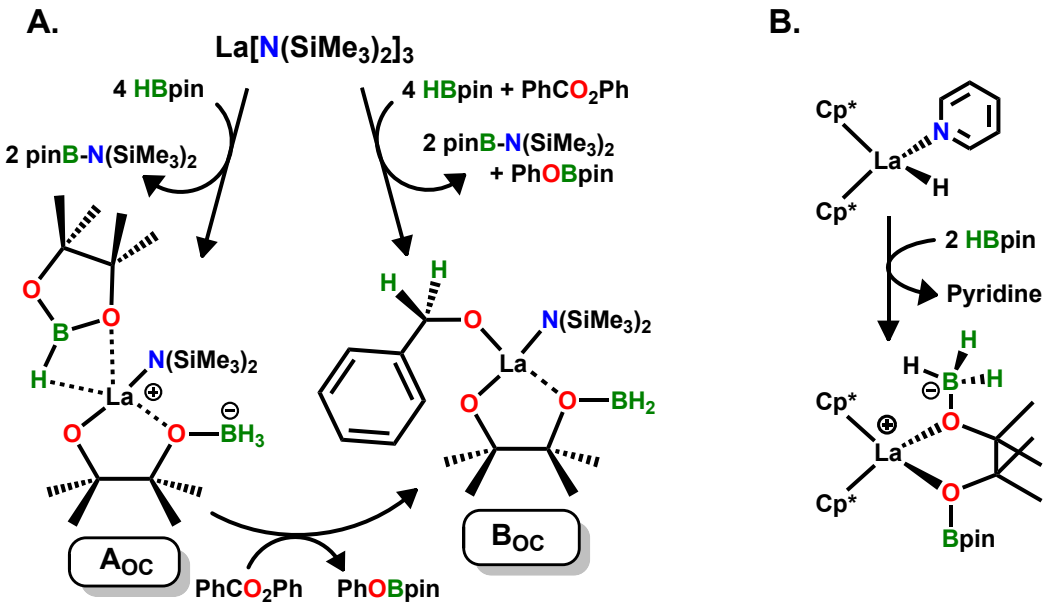

Scheme 2. **A**. Catalyst off-cycle products observed in NMR studies of stoichiometric substrate and La^{NTMS}. **B**. Structure of a product similar to A_{OC} isolated from an organolanthanide-catalyzed pyridine dearomatization/hydroboration process.[17] Cp* = η^5-pentamethylcyclopentadienyl

maintained, as evidenced by a greater downfield shift in the adjacent $C(CH_3)_2$ protons (1.56 ppm),[18] whereas with pyridine hydroboration, this bond is broken and replaced by an intact Bpin moiety (adjacent $C(CH_3)_2$ protons appear at 1.30 ppm; Scheme 2B). When ester is added to complex A_{OC}, or when stoichiometric ester and HBpin are added simultaneously to La^{NTMS}, the ^{11}B NMR signal at -6.3 ppm disappears and a triplet at 47.4 ppm grows in, indicating a hydride is transferred from the $R\text{-}BH_3^-$ group, yielding $R\text{-}BH_2$ and a partially reduced ester (B_{OC}, Scheme 2A). Subsequent addition of excess substrates does not result in turnover, indicating this is, in fact, an off-cycle pathway that likely results in deactivation. We propose that the true active catalyst (*vide infra*) is not detectable by NMR, likely due to the availability of the above deactivation pathway at low substrate concentrations relative to catalyst concentration (such as those employed in the above spectroscopic studies). Attempts to more fully characterize these off-cycle products were unsuccessful due to their decomposition into intractable, white solids over the course of 2

hours at room temperature. However, DFT analysis argues that these products are energetically accessible in the conditions employed above and their formation is highly exergonic (see SI, p. S17).

DFT Mechanistic Analysis

To more fully understand the mechanism of La^{NTMS}-catalyzed ester reduction with pinacolborane, DFT modeling of the catalyst activation process, catalytic cycle, and potential off-cycle pathways was performed using methyl benzoate as a model ester (see Experimental Section for computational details; see SI for DFT analysis and free energy profiles of the catalyst deactivation pathway). Figure 4 shows the computed catalyst activation process. The La^{NTMS} pre-catalyst is activated for ester reduction first by HBpin-mediated cleavage of a La-N$(SiMe_3)_2$ bond (**TS_{act}-1**), forming complex **Iact-2**. Direct hydride transfer from the coordinated $[(SiMe_3)_2NB(H)pin]^-$ molecule of **Iact-2** to a coordinated ester molecule (**TS_{act}-2**) then affords lanthanide-hemiacetal species **I_{act}-3** and pinB-N$(SiMe_3)_2$ as a byproduct. Subsequent coordination of a second HBpin molecule leads to the active catalyst. The entire process is exergonic (-44.9 kcal/mol) and has an energy barrier of only 9.9 kcal/mol associated with the scission of the La-N

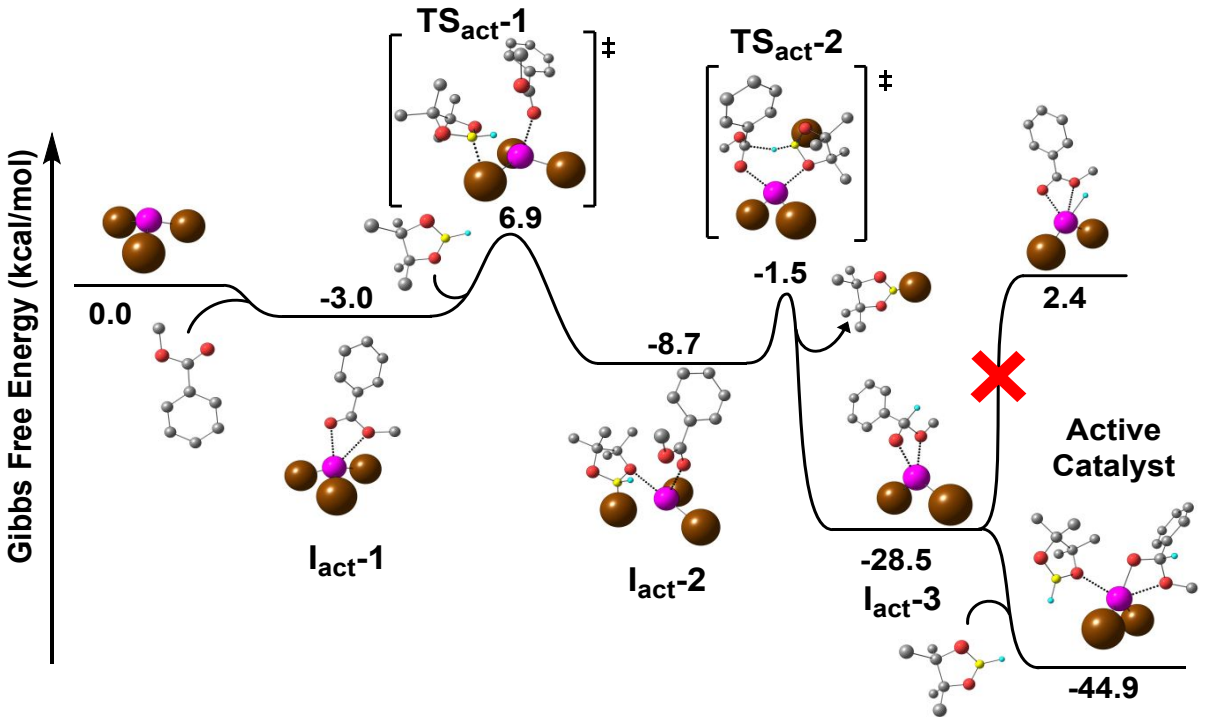

Figure 4. Gibbs free energy profile (kcal/mol) of the La^{NTMS} pre-catalyst activation process using methyl benzoate as a model ester substrate. The occurrence of a La-centered hydride (via the step denoted by a red "X") is energetically implausible. La = violet, C = grey, H = cyan, B = yellow, and $N[SiMe_3]_2$ = brown.

bond in **TS_{act}-1**. The possibility of a $[(Me_3Si)_2N]_2$La-H active catalyst was also explored due to the ubiquity of proposed L_2Ln-H species as both active catalysts and intermediates in the organolanthanide literature,[17, 19] however the energy required to form such a species in the present system (> 30kcal/mol) appears to be unlikely.

The proposed catalytic cycle consists of three principal steps (Figure 5): 1) Lewis acidic boron (of the coordinated HBpin molecule) attack on the hemiacetal oxygen of the active catalyst **A** (**TS1**), leading to formation of a new B-O bond and dissociation of the La-$O_{hemiacetal}$ bond. This step, which produces a La-coordinated hemiacetal-pinacolborate species, proceeds with a computed barrier of 3.1 kcal/mol, and the subsequent coordination of a second ester molecule leads to an overall stabilization (-12.4 kcal/mol) and generates complex **B**. 2) Transfer of the ester

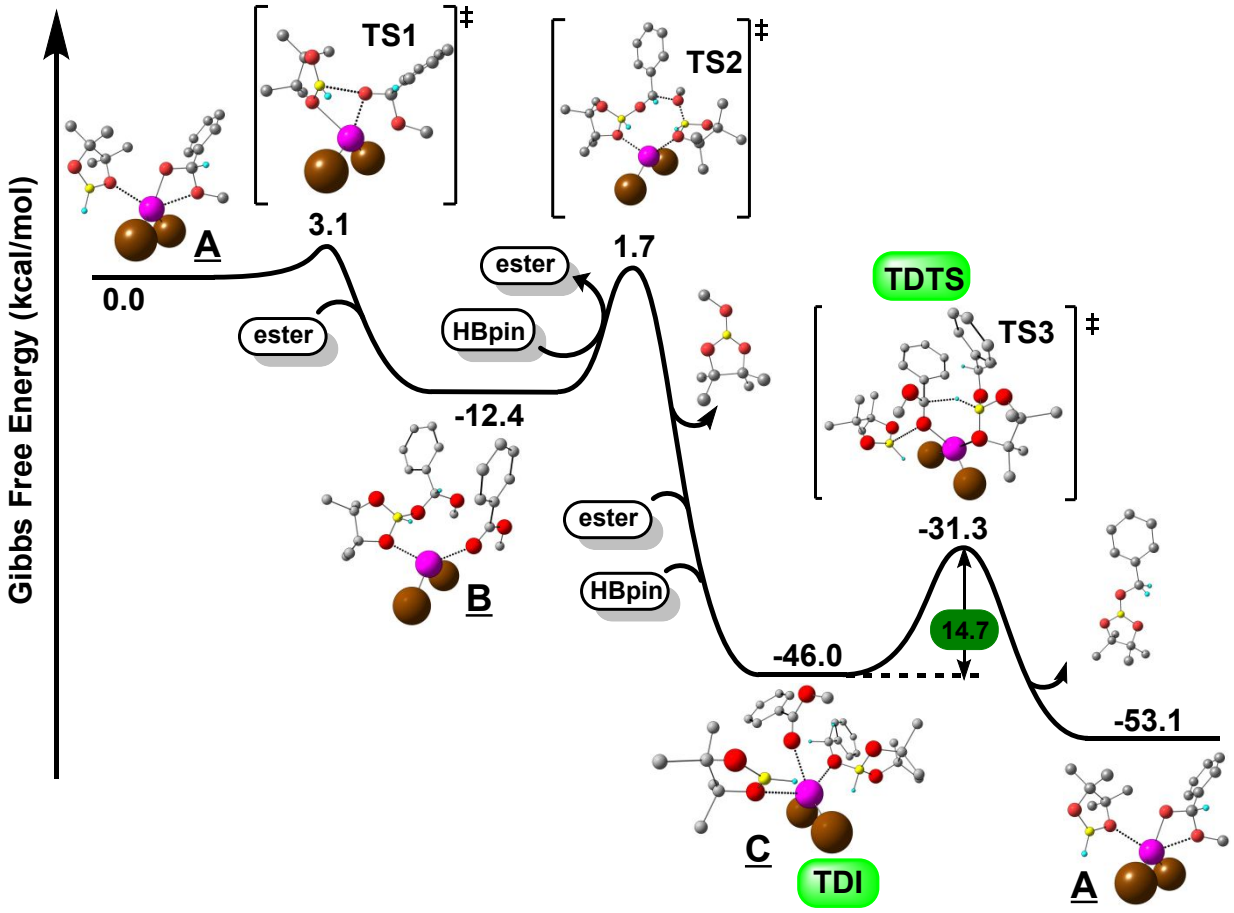

Figure 5. Gibbs free energy profile (kcal/mol) for the catalytic cleavage of methyl benzoate via hydroboration. The active catalyst is derived from La^{NTMS} (Figure 4); TDI = turnover-determining intermediate, TDTS = turnover-determining transition state. La = violet, C = grey, H = cyan, B = yellow, and $N[SiMe_3]_2$ = brown.

methoxy group to the coordinated HBpin, followed by a rapid hydride transfer from $[HB(OMe)(pin)]^-$ to the La-hydroborate complex (**TS2**), forms the first reduction product, MeOBpin. The product of this step (complex **C**) is highly stabilized by the coordination of both ester and HBpin molecules, leading to an overall stabilization of -46.0 kcal/mol. 3) Intramolecular hydride transfer from complex **C** to the coordinated ester (**TS3**) leads to formation and subsequent release of the second reduction product, $PhCH_2OBpin$, restoring the active catalyst **A**. In the

transition state structure, HBpin loses its coordination with the La metal center and interacts weakly with the carbonyl oxygen of the coordinated ester. This step is exergonic (-7.1 kcal/mol) and represents the rate-determining step with an energy barrier of 14.7 kcal/mol.

Discussion

Figure 6 presents a plausible scenario that accounts for the experimental mechanistic observations and DFT calculations discussed above. Note that negligible reaction is observed in stoichiometric mixtures of La^{NTMS} and phenyl benzoate, providing evidence that La^{NTMS} must be

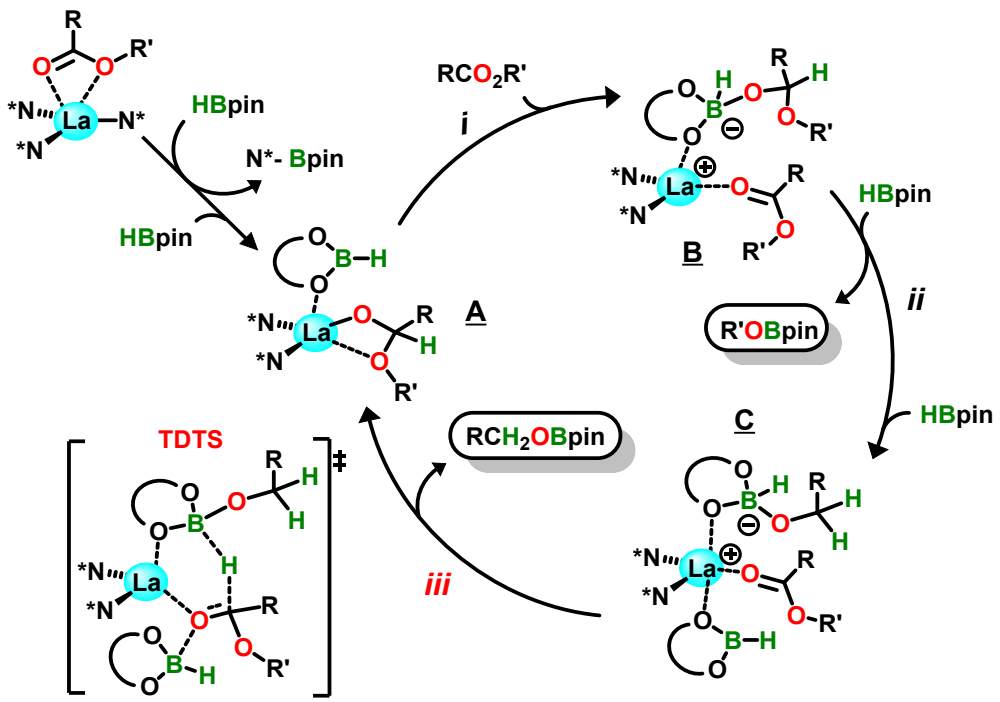

Figure 6. Catalyst activation and catalytic cycle for La^{NTMS}-catalyzed ester hydroboration. N* = $N(SiMe_3)_2$. Step ***iii*** is proposed to be turnover limiting, and the DFT-computed turnover-determining transition state (TDTS) is shown.

activated with HBpin to initiate the catalytic reduction cycle. According to the DFT and NMR results described above, activation of the ester-coordinated precatalyst with HBpin, followed by coordination of additional HBpin, generates the lanthanide-hemiacetal active catalyst **A** and known pinB-$N(SiMe_3)_2$ as a by-product. Just as in the stoichiometric studies described above, the

TMS methyl protons of the aminoborane are also observed in the *in situ* ^{1}H NMR spectra of catalytic reactions (the Bpin methyl protons are obscured by substrate/product signals).[16] This resonance integrates in an approximate 1:2 ratio to the La^{NTMS} methyl protons (at δ 0.28 ppm), arguing mono-activation of the pre-catalyst does in fact occur. Furthermore, Sadow and co-workers recently proposed a similar hemiacetal-based catalytic intermediate, [La]-OCHR(OR), for $La[C(SiHMe_2)_3]_3$-catalyzed ester hydroboration based on detailed kinetic studies.[7a] The similarities between these homoleptic lanthanide complexes, both in terms of structure and reactivity, suggest similar species would be active for ester hydroboration. Additionally, the involvement of both ester *and* HBpin in catalyst activation is supported in the present work by the off-cycle reaction observed when HBpin is allowed to react with La^{NTMS} in the absence of ester (*vide supra*). This suggests that without a substantial excess of ester (relative to La^{NTMS}) to accept the hydride from La-coordinated HBpin and generate **A**, an unstable La-hydride/borate species is formed, opening the pinacolate ring of HBpin and deactivating the La center.[17]

Activated by the oxophilic La center, HBpin promotes La-$O_{hemiacetal}$ bond dissociation and B-$O_{hemiacetal}$ bond formation (Figure 6, step *i*), producing a transient complex that is spontaneously stabilized by coordination of a new ester molecule, yielding intermediate **B**. This sterically congested species then rearranges intramolecularly, yielding R'OBpin. Subsequent, barrierless coordination of HBpin affords stabilized complex **C** (step *ii*). Finally, intramolecular hydride transfer from the boron atom of the hydroborate-La complex to the coordinated ester (step ***iii***) restores the active catalyst **A** for subsequent catalytic cycles. Assignment of this step as turnover-limiting is supported by several experimental observations. The experimentally derived activation parameters, consisting of a small, positive $\Delta H^{\ddagger}$ and large, negative $\Delta S^{\ddagger}$, suggest the transition state is highly organized and sterically congested, and the overall first-order reaction rate requires that

the turnover-limiting step is intramolecular.[20] Notably, the activation parameters reported for this system ($\Delta H^{\ddagger}$ = 8.2 kcal/mol, $\Delta S^{\ddagger}$ = -53.1 e.u.) are very similar to those reported previously for aldehyde hydroboration with B-alkyl-9-BBN ($\Delta H^{\ddagger}$ = 9.1 - 9.8 kcal/mol, $\Delta S^{\ddagger}$ = -43 - -49 e.u.).[21] The transition state proposed for this reaction is also quite similar to the one proposed above, as it proceeds through a sterically congested and conformationally constrained transition state and involves intramolecular hydride transfer to the carbonyl.

The zero order reaction rate law found experimentally for HBpin and ester concentrations is supported by the DFT calculations (Figure 5), which find that neither HBpin nor ester enters the catalytic cycle between the turnover-determining intermediate (TDI, **C**) and the turnover-determining transition state (TDTS, **TS3**).[22] The high degree of steric congestion in the transition state would lead to depressed rates for sterically encumbered substrates, which is observed experimentally. A small, positive Hammett ρ value (ρ = 1.11, Figure 2) indicates that the transition state is stabilized by withdrawal of electron density from the carbonyl carbon, but to a much lesser extent than is observed for typical base-catalyzed ester cleavages (ρ =1.9-2.5).[23] This supports the present assignment that the turnover-limiting step involves nucleophilic hydride attack on a carbonyl bond that has been activated, in this case by simultaneous C=O coordination to both HBpin and La, priming the acyl carbon for nucleophilic attack and diminishing ρ.

While the present KIE of 1.49 for ester reduction with DBpin is small for a primary KIE, it is much larger than typical values for secondary isotope effects, [20] supporting an assignment of B-H scission in the turnover-limiting step. While the lack of previously reported KIEs for HBpin-based ester reduction prevents direct comparison, analogous reductions of N-heteroarenes,[24] ketones,[25] and nitriles[26] proceed with somewhat higher KIEs, ranging from 2.3-2.8. However, Hartwig and co-workers report a similarly small KIE (1.62) for the addition of catecholborane, via σ-bond

metathesis, to a Ru-alkyl, indicating KIEs this small are not without precedent for B-H bond scission.[27] In this system, it is likely that slight O→B interaction in the TDTS likely weakens the B-H bond prior to scission, contributing to the lower KIE than might be expected for such a reaction. The terminal location of the borane derived hydrogens is also telling. As noted above, the deuterium-labelling experiment shows that both hydride equivalents are delivered to the carbonyl carbon, effectively ruling out the possibility of a reverse-Tishchenko-based mechanism (Scheme 3). Such a mechanism warrants consideration since the Tishchenko reaction (coupling of aldehydes to form esters) is catalyzed by Ln^{NTMS} complexes,[28] and a similar mechanism was proposed previously for Mg-catalyzed ester hydroboration.[7d] Note also that a Tishchenko-like pre-equilibrium could not account for substrates lacking an α-H in the R' position (i.e., Table 1, entries 1, 3, and 5) since the aldehyde C=O bond cannot form at a fully substituted carbon center.

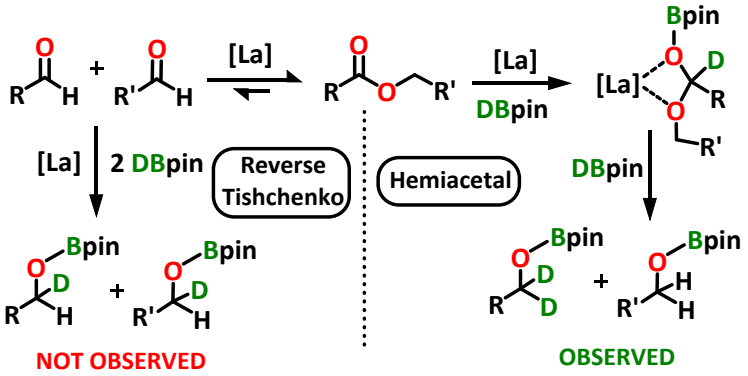

Scheme 3. Isotopic labelling differentiation of the hemiacetal-based ester hydroboration mechanism proposed here and the reverse-Tishchenko type mechanism proposed for Mg-catalyzed ester hydroboration.[7d]

Conclusions

The scope and mechanism of La^{NTMS}-catalyzed, pinacolborane-based reduction of a diverse series of esters is investigated experimentally and by DFT computation. The catalyst shows complete selectivity for ester reduction over competing nitro groups, alkenes, and alkynes, even at

temperatures as high as 60°C. Experimental and computation-based mechanistic studies indicate that the active catalyst is generated from the La^{NTMS} pre-catalyst by HBpin-mediated La-N bond scission, generating a La-hemiacetal species that is active for ester reduction. The presence of ester in the catalyst activation process likely inhibits the formation of a L_2La-H species, which could explain the selectivity of this catalyst over alkene and alkyne hydroboration, reactions which have previously been proposed to proceed through a L_2La-H active catalyst.[13k, 19e] The turnover-limiting step is proposed to involve intramolecular, concerted hydride transfer/C-O bond cleavage, leading to an overall first-order rate law, rate = $[La^{NTMS}]^1[ester]^0[HBpin]^0$. This report further demonstrates the important role that lanthanide catalysis can play in experimental chemical synthesis, and it represents the first attempt at a combined experimental-theoretical approach to discerning HBpin-mediated ester reduction. By combining a mild reductant like HBpin with the highly active and readily accessible catalyst La^{NTMS}, a safer, more selective, and convenient route to ester reduction has been realized.

Experimental Section

Materials and Methods

All manipulations of air-sensitive materials were carried out with rigorous exclusion of O_2 and moisture in flame- or oven-dried Schlenk-type glassware on a dual-manifold Schlenk line or in an argon-filled glovebox with a high capacity recirculator (<0.5 ppm O_2). Benzene-d_6 (Cambridge Isotope Laboratories; 99+ atom % D) was stored over Na/K alloy and vacuum transferred prior to use. $La[N(SiMe_3)_2]_3$ (La^{NTMS}) and hexamethylbenzene were purchased from Sigma-Aldrich Co. and sublimed under high-vacuum (10^{-6} Torr). Pinacolborane ("HBpin") was purchased from Sigma-Aldrich Co. and distilled under high-vacuum (10^{-6} Torr) to remove trace boronic acid impurities and stored at -35°C in a glovebox.[17] Ester substrates were purchased from

Sigma-Aldrich Co. and dried over 3Å molecular sieves (liquid esters) or under vacuum overnight (solid esters). The products of ester cleavage (alkoxy boryl esters) were characterized by ^{1}H, ^{13}C, and ^{11}B NMR. NMR spectra were recorded on a Bruker Avance III (500 MHz, ^{1}H; 125 MHz, ^{13}C), Varian Inova 500 (500 MHz, ^{1}H; 125 MHz, ^{13}C), Agilent DD MR-400 (400 MHz, ^{1}H; 100 MHz, ^{13}C; 128 MHz, ^{11}B), or Agilent DD2 500 (500 MHz, ^{1}H; 125 MHz, ^{13}C). Chemical shifts (δ) for ^{1}H and ^{13}C are referenced to residual solvent resonances (7.16 and 128.06 ppm, resp., for benzene-d_6). ^{11}B shifts are referenced to an external $BF_3{\cdot}OEt_2$ standard. NMR scale reactions were carried out either in Teflon-sealed J. Young tubes or rubber septum-sealed tubes.

General Procedure for NMR-scale, LaNTMS-catalyzed ester reductions with HBpin

For solid esters: In the glovebox, the ester substrate (0.25 mmol) and HBpin (0.55 mmol) were dissolved in benzene-d_6 (total volume 1.0 mL). This solution was then injected into a vial containing La^{NTMS} (2.5 μmol) and shaken to dissolve the catalyst. The reaction mixture was next transferred to a J. Young capped NMR tube and removed from the glovebox, and the ensuing reaction was monitored by ^{1}H NMR.

For liquid esters: In a glovebox, La^{NTMS} (2.5 μmol) was placed in a rubber septum-sealed NMR tube, and the cap was wrapped with Parafilm. HBpin (0.55 mmol) and benzene-d_6 were next added to a septum-sealed vial, and the cap was wrapped with electrical tape. Outside the glovebox, the liquid ester (0.25 mmol) was then injected into the vial with HBpin and internal standard, the vial was shaken, and the contents were injected into the NMR tube containing the catalyst, all under N_2. The tube was shaken to dissolve the catalyst, and the ensuing reaction was monitored by ^{1}H NMR.

DBpin Synthesis

This synthesis was adapted from literature procedures.[29] BD_3•SMe_2 (Cambridge Isotope Laboratories, 8.5 mmol, 10 *M*) was diluted with 10 mL DCM in an addition funnel under N_2. This solution was next added dropwise over 30 min to a 0°C solution of pinacol (8.5 mmol, 1.0 g) in 20 mL DCM. After addition was complete, the solution was brought to room temperature and stirred until bubbling was no longer observed (1 h). The DBpin was purified by distillation (0°C at 10 mmHg). ^{1}H NMR (400 MHz, C_6D_6): 1.00 (s, 12H, DB*pin*) ^{11}B NMR (128 MHz, C_6D_6): 28.37 (t, $^2J_{DB}$=22.8 Hz).

Computational Details

Geometry optimizations of all reactants, products, intermediates, and transition states were carried out along the entire catalytic cycle. Calculations were performed adopting the M06 hybrid meta-GGA functional. The effective core potential of Hay and Wadt[30], (LANL2DZ) and the relative basis set were used for the La and Si atoms. The standard all-electron 6-31G** basis[31] was used for all the remaining atoms. Molecular geometry optimization of stationary points was carried out without symmetry constraints and used analytical gradient techniques. The transition states were searched with the "distinguished reaction coordinate procedure" along the emerging bonds. Step *i* of Figure 4 was monitored along the emerging C–O bond, whereas the subsequent bond formation/breaking step induced by the approach of a second HBpin molecule (step *ii*) was monitored along the breaking C–O bond. Finally, the hydride transfer of step *iii* and the catalyst activation step were monitored along the emerging C-H bond. Methyl benzoate was adopted as substrate model. Frequency analysis was performed to obtain thermochemical information about the reaction pathways at 298 K using the harmonic approximation. The difference in translational and rotational Gibbs free energy when moving from gas to solvent are accounted for by adding an energy contribution of 8RT to each species as detailed in the literature.[32] Moreover, the effect of

concentration on moving from 1 atm to 1 *M* is accounted for by adding an energy contribution of 1.89 kcal/mol ($RTln(P_{1M}/P_{1atm})$) to each species. All calculations were performed using the G16 code[33] on Linux cluster systems.

AUTHOR INFORMATION

Corresponding Author

t-marks@northwestern.edu, tracy.lohr@shell.com

Present Addresses

‡ Shell Projects & Technology, Shell Technology Center Houston, 3333 Highway 6 South, Houston, Texas, 77082, United States.

Author Contributions

The manuscript was written through contributions of all authors. All authors have given approval to the final version of the manuscript.

Notes

The authors declare no competing financial interest.

ASSOCIATED CONTENT

Supporting Information. The following file is available free of charge.

Experimental details, kinetic and thermodynamic data, computation details, product characterization and NMR spectra. (Word)

ACKNOWLEDGMENTS

The authors thank the National Science Foundation (grants CHE-1464488 and CHE-1856619) for financial support. This work made use of the IMSERC facility at Northwestern University, which has received support from the NSF (CHE-1048773 and CHE-9871268); Soft and Hybrid

Nanotechnology Experimental (SHyNE) Resource (NSF NNCI-1542205); the State of Illinois and International Institute for Nanotechnology. V.L.W. thanks NSF for an NSF Graduate Research Fellowship. Computational resources were provided by the Northwestern University Quest High Performance Computing cluster (T.L.L.) and CINECA award N. HP10CP3HMF 2017 under the ISCRA initiative (A.M.).

REFERENCES

1. (a) Cornils, B.; Hermann, W. A.; Beller, M.; Paciello, R., *Applied Homogeneous Catalysis with Organometallic Compounds: A Comprehensive Handbook in Four Volumes, Volume 4*. Wiley-VCH Verlag GmbH & Co: Weinheim, Germany, 2017; (b) Andersson, P. G.; Munslo, I. J., In *Modern Reduction Methods*, Wiley: New York, 2008; (c) Roberts, S. M.; Whittall, J., *Regio- and Stereo-Controlled Oxidations and Reductions*. John Wiley & Sons: West Sussex, England, 2007; Vol. 5; (d) Otera, J., *Modern Carbonyl Chemistry*. Wiley-VCH: Weinheim, Germany, 2000.

2. Magano, J.; Dunetz, J. R. Large-Scale Carbonyl Reductions in the Pharmaceutical Industry. *Org. Proc. Res. Dev.* **2012,** *16*, 1156-1184.

3. (a) Lohr, T. L.; Li, Z.; Marks, T. J. Thermodynamic Strategies for C–O Bond Formation and Cleavage via Tandem Catalysis. *Acc. Chem. Res.* **2016,** *49*, 824-834; (b) Wu, L.; Moteki, T.; Gokhale, A. A.; Flaherty, D. W.; Toste, F. D. Production of Fuels and Chemicals from Biomass: Condensation Reactions and Beyond. *Chem* **2016,** *1*, 32-58; (c) Hu, C.; Creaser, D.; Siahrostami, S.; Grönbeck, H.; Ojagh, H.; Skoglundh, M. Catalytic hydrogenation of C=C and C=O in unsaturated fatty acid methyl esters. *Catal. Sci. Tech.* **2014,** *4*, 2427-2444; (d) Turek, T.; Trimm, D. L. The Catalytic Hydrogenolysis of Esters to Alcohols. *Cat. Rev. - Sci. Eng.* **1994,** *36*, 645-683.

4. (a) Smith, M., *March's Advanced Organic Chemistry: Reactions, Mechanisms, and Structure*. Wiley: Hoboken, 2013; (b) Seyden-Penne, J., *Reductions by the Alumino- and Borohydrides in Organic Synthesis*. 2nd ed.; Wiley-VCH: Weinheim, Germany, 1997; (c) Brown, H. C.; Krishnamurthy, S. Forty years of hydride reductions. *Tetrahedron* **1979,** *35*, 567-607; (d) Nystrom, R. F.; Brown, W. G. Reduction of Organic Compounds by Lithium Aluminum Hydride. III. Halides, Quinones, Miscellaneous Nitrogen Compounds1. *J. Am. Chem. Soc.* **1948,** *70*, 3738-3740.

5. (a) Liu, W.; Sahoo, B.; Junge, K.; Beller, M. Cobalt Complexes as an Emerging Class of Catalysts for Homogeneous Hydrogenations. *Acc. Chem. Res.* **2018,** *51*, 1858-1869; (b) Pritchard, J.; Filonenko, G. A.; van Putten, R.; Hensen, E. J. M.; Pidko, E. A. Heterogeneous and homogeneous catalysis for the hydrogenation of carboxylic acid derivatives: history, advances and future directions. *Chem. Soc. Rev.* **2015,** *44*, 3808-3833; (c) Chakraborty, S.; Bhattacharya, P.; Dai, H.; Guan, H. Nickel and Iron Pincer Complexes as Catalysts for the Reduction of Carbonyl Compounds. *Acc. Chem. Res.* **2015,** *48*, 1995-2003; (d) Werkmeister, S.; Junge, K.; Beller, M. Catalytic Hydrogenation of Carboxylic Acid Esters, Amides, and Nitriles with Homogeneous Catalysts. *Org. Proc. Res. Dev.* **2014,** *18*, 289-302; (e) Saudan, L. A., Hydrogenation of Esters. In *Sustainable Catalysis*, Dunn, P. J.; Hii, K. K.; Krische, M. J.; Williams, M. T., Eds. 2013; (f) Clarke, M. L. Recent developments in the homogeneous hydrogenation of carboxylic acid esters. *Catal. Sci. Tech.* **2012,** *2*, 2418-2423; (g) Dub, P. A.; Ikariya, T. Catalytic Reductive Transformations of Carboxylic and Carbonic Acid Derivatives Using Molecular Hydrogen. *ACS Catal.* **2012,** *2*, 1718-1741.

6. (a) Andrews, R. J.; Chitnis, S. S.; Stephan, D. W. Carbonyl and olefin hydrosilylation mediated by an air-stable phosphorus(iii) dication under mild conditions. *Chem. Commun.* **2019,**

55, 5599-5602; (b) Gebbink, R. J. M. K.; Moret, M.-E., *Non-Noble Metal Catalysis: Molecular Approaches and Reactions*. Wiley-VCH: Weinheim, Germany, 2019; (c) Raya-Barón, Á.; Oña-Burgos, P.; Fernández, I. Iron-Catalyzed Homogeneous Hydrosilylation of Ketones and Aldehydes: Advances and Mechanistic Perspective. *ACS Catal.* **2019**, *9*, 5400-5417; (d) Ritter, F.; Mukherjee, D.; Spaniol, T. P.; Hoffmann, A.; Okuda, J. A Masked Cuprous Hydride as a Catalyst for Carbonyl Hydrosilylation in Aqueous Solutions. *Angew. Chem. Int. Ed.* **2019,** *58*, 1818-1822; (e) Zhou, Y.; Khan, R.; Fan, B.; Xu, L. Ruthenium-Catalyzed Selective Reduction of Carboxylic Esters and Carboxamides. *Synthesis* **2019,** *51*, 2491-2505; (f) Rock, C. L.; Groy, T. L.; Trovitch, R. J. Carbonyl and ester C–O bond hydrosilylation using κ^4-diimine nickel catalysts. *Dalton Trans.* **2018,** *47*, 8807-8816; (g) Kelly, C. M.; McDonald, R.; Sydora, O. L.; Stradiotto, M.; Turculet, L. A Manganese Pre-Catalyst: Mild Reduction of Amides, Ketones, Aldehydes, and Esters. *Angew. Chem. Int. Ed.* **2017,** *56*, 15901-15904; (h) Trovitch, R. J. The Emergence of Manganese-Based Carbonyl Hydrosilylation Catalysts. *Acc. Chem. Res.* **2017,** *50*, 2842-2852; (i) Süsse, L.; Hermeke, J.; Oestreich, M. The Asymmetric Piers Hydrosilylation. *J. Am. Chem. Soc.* **2016,** *138*, 6940-6943; (j) Lampland, N. L.; Pindwal, A.; Neal, S. R.; Schlauderaff, S.; Ellern, A.; Sadow, A. D. Magnesium-catalyzed hydrosilylation of α,β-unsaturated esters. *Chem. Sci.* **2015,** *6*, 6901-6907; (k) Trovitch, R. J. Comparing Well-Defined Manganese, Iron, Cobalt, and Nickel Ketone Hydrosilylation Catalysts. *Synlett* **2014,** *25*, 1638-1642; (l) Addis, D.; Das, S.; Junge, K.; Beller, M. Selective Reduction of Carboxylic Acid Derivatives by Catalytic Hydrosilylation. *Angew. Chem. Int. Ed.* **2011,** *50*, 6004-6011; (m) Zhang, M.; Zhang, A. Iron-catalyzed hydrosilylation reactions. *Appl. Organomet. Chem.* **2010,** *24*, 751-757; (n) Yang, J.; Tilley, T. D. Efficient Hydrosilylation of Carbonyl Compounds with the Simple Amide Catalyst $[Fe\{N(SiMe_3)_2\}_2]$. *Angew. Chem. Int. Ed.* **2010,** *49*, 10186-10188; (o) Marciniec, B., *Hydrosilylation: A*

Comprehensive Review on Recent Advances. Springer: Berlin, 2009; (p) Díez-González, S.; Nolan, S. P. Transition Metal-Catalyzed Hydrosilylation of Carbonyl Compounds and Imines. A Review. *Org. Prep. Proced. Int.* **2007,** *39*, 523-559; (q) Roy, A. K., A Review of Recent Progress in Catalyzed Homogeneous Hydrosilation (Hydrosilylation). In *Adv. Organomet. Chem.*, West, R.; Hill, A. F.; Fink, M. J., Eds. Academic Press: 2007; Vol. 55, pp 1-59.

7. (a) Patnaik, S.; Sadow, A. D. Interconverting Lanthanum Hydride and Borohydride Catalysts for C=O Reduction and C−O Bond Cleavage. *Angew. Chem. Int. Ed.* **2019,** *58,* 2505-2509; (b) Barman, M. K.; Baishya, A.; Nembenna, S. Magnesium amide catalyzed selective hydroboration of esters. *Dalton Trans.* **2017,** *46*, 4152-4156; (c) Mukherjee, D.; Shirase, S.; Spaniol, T. P.; Mashima, K.; Okuda, J. Magnesium hydridotriphenylborate $[Mg(thf)_6][HBPh_3]_2$: a versatile hydroboration catalyst. *Chem. Commun.* **2016,** *52*, 13155-13158; (d) Mukherjee, D.; Ellern, A.; Sadow, A. D. Magnesium-catalyzed hydroboration of esters: evidence for a new zwitterionic mechanism. *Chem. Sci.* **2014,** *5*, 959-964; (e) Khalimon, A. Y.; Farha, P.; Kuzmina, L. G.; Nikonov, G. I. Catalytic hydroboration by an imido-hydrido complex of Mo(IV). *Chem. Commun.* **2012,** *48*, 455-457; (f) Arrowsmith, M.; Hill, M. S.; Hadlington, T.; Kociok-Köhn, G.; Weetman, C. Magnesium-Catalyzed Hydroboration of Pyridines. *Organometallics* **2011,** *30*, 5556-5559.

8. Obligacion, J. V.; Chirik, P. J. Earth-abundant transition metal catalysts for alkene hydrosilylation and hydroboration. *Nature Reviews Chemistry* **2018,** *2*, 15-34.

9. *For a review, see:* (a) Chong, C. C.; Kinjo, R. Catalytic Hydroboration of Carbonyl Derivatives, Imines, and Carbon Dioxide. *ACS Catal.* **2015,** *5*, 3238-3259; *For selected, recent examples, see:* (b) Dasgupta, R.; Das, S.; Hiwase, S.; Pati, S. K.; Khan, S. N-Heterocyclic

Germylene and Stannylene Catalyzed Cyanosilylation and Hydroboration of Aldehydes. *Organometallics* **2019,** *38*, 1429-1435; (c) Kuciński, K.; Hreczycho, G. Lithium triethylborohydride as catalyst for solvent-free hydroboration of aldehydes and ketones. *Green Chemistry* **2019,** *21*, 1912-1915; (d) Woodside, A. J.; Smith, M. A.; Herb, T. M.; Manor, B. C.; Carroll, P. J.; Rablen, P. R.; Graves, C. R. Synthesis and Characterization of a Tripodal Tris(nitroxide) Aluminum Complex and Its Catalytic Activity toward Carbonyl Hydroboration. *Organometallics* **2019,** *38*, 1017-1020; (e) Baishya, A.; Baruah, S.; Geetharani, K. Efficient hydroboration of carbonyls by an iron(ii) amide catalyst. *Dalton Trans.* **2018,** *47*, 9231-9236; (f) Das, U. K.; Higman, C. S.; Gabidullin, B.; Hein, J. E.; Baker, R. T. Efficient and Selective Iron-Complex-Catalyzed Hydroboration of Aldehydes. *ACS Catal.* **2018,** *8*, 1076-1081; (g) Ghatak, T.; Makarov, K.; Fridman, N.; Eisen, M. S. Catalytic regeneration of a Th–H bond from a Th–O bond through a mild and chemoselective carbonyl hydroboration. *Chem. Commun.* **2018,** *54*, 11001-11004; (h) Chen, S.; Yan, D.; Xue, M.; Hong, Y.; Yao, Y.; Shen, Q. Tris(cyclopentadienyl)lanthanide Complexes as Catalysts for Hydroboration Reaction toward Aldehydes and Ketones. *Org. Lett.* **2017,** *19*, 3382-3385; (i) Huang, Z.; Liu, D.; Camacho-Bunquin, J.; Zhang, G.; Yang, D.; López-Encarnación, J. M.; Xu, Y.; Ferrandon, M. S.; Niklas, J.; Poluektov, O. G.; Jellinek, J.; Lei, A.; Bunel, E. E.; Delferro, M. Supported Single-Site Ti(IV) on a Metal–Organic Framework for the Hydroboration of Carbonyl Compounds. *Organometallics* **2017,** *36*, 3921-3930; (j) Schneider, J.; Sindlinger, C. P.; Freitag, S. M.; Schubert, H.; Wesemann, L. Diverse Activation Modes in the Hydroboration of Aldehydes and Ketones with Germanium, Tin, and Lead Lewis Pairs. *Angew. Chem. Int. Ed.* **2017,** *56*, 333-337; (k) Vasilenko, V.; Blasius, C. K.; Wadepohl, H.; Gade, L. H. Mechanism-Based Enantiodivergence in Manganese Reduction Catalysis: A Chiral Pincer Complex for the Highly Enantioselective Hydroboration of Ketones.

Angew. Chem. Int. Ed. **2017,** *56*, 8393-8397; (l) Weidner, V. L.; Barger, C. J.; Delferro, M.; Lohr, T. L.; Marks, T. J. Rapid, Mild, and Selective Ketone and Aldehyde Hydroboration/Reduction Mediated by a Simple Lanthanide Catalyst. *ACS Catal.* **2017,** *7*, 1244-1247; (m) Wu, D.; Wang, R.; Li, Y.; Ganguly, R.; Hirao, H.; Kinjo, R. Electrostatic Catalyst Generated from Diazadiborinine for Carbonyl Reduction. *Chem* **2017,** *3*, 134-151; (n) Manna, K.; Ji, P.; Greene, F. X.; Lin, W. Metal–Organic Framework Nodes Support Single-Site Magnesium–Alkyl Catalysts for Hydroboration and Hydroamination Reactions. *J. Am. Chem. Soc.* **2016,** *138*, 7488-7491.

10. (a) Lohr, T. L.; Li, Z.; Assary, R. S.; Curtiss, L. A.; Marks, T. J. Mono- and tri-ester hydrogenolysis using tandem catalysis. Scope and mechanism. *Energ. Environ. Sci.* **2016,** *9*, 550-564; (b) Lohr, T. L.; Li, Z.; Assary, R. S.; Curtiss, L. A.; Marks, T. J. Thermodynamically Leveraged Tandem Catalysis for Ester RC(O)O–R′ Bond Hydrogenolysis. Scope and Mechanism. *ACS Catal.* **2015,** *5*, 3675-3679; (c) Lohr, T. L.; Li, Z.; Marks, T. J. Selective Ether/Ester C–O Cleavage of an Acetylated Lignin Model via Tandem Catalysis. *ACS Catal.* **2015,** *5*, 7004-7007.

11. (a) Schuetz, S. A.; Day, V. W.; Sommer, R. D.; Rheingold, A. L.; Belot, J. A. Anhydrous Lanthanide Schiff Base Complexes and Their Preparation Using Lanthanide Triflate Derived Amides. *Inorg. Chem.* **2001,** *40*, 5292-5295; (b) Bradley, D. C.; Ghotra, J. S.; Hart, F. A. Three-co-ordination in lanthanide chemistry: tris[bis(trimethylsilyl)amido]lanthanide(III) compounds. *J. Chem. Soc., Chem. Commun.* **1972**, 349-350; (c) Alyea, E. C.; Bradley, D. C.; Copperthwaite, R. G. Three-co-ordinated transition metal compounds. Part I. The preparation and characterization of tris(bistrimethylsilylamido)-derivatives of scandium, titanium, vanadium, chromium, and iron. *J. Chem. Soc., Dalton Trans.* **1972**, 1580-1584.

12. (a) Edelmann, F. T. Lanthanides and actinides: Annual survey of their organometallic chemistry covering the year 2017. *Coord. Chem. Rev.* **2018,** *370*, 129-223; (b) Qian, Q.; Zhu, W.; Lu, C.; Zhao, B.; Yao, Y. Asymmetric Michael addition of malonates to unsaturated ketones catalyzed by rare earth metal complexes bearing phenoxy functionalized chiral diphenylprolinolate ligands. *Tetrahedron: Asymmetry* **2016,** *27*, 911-917; (c) Wang, C.; Huang, L.; Lu, M.; Zhao, B.; Wang, Y.; Zhang, Y.; Shen, Q.; Yao, Y. Anionic phenoxy-amido rare-earth complexes as efficient catalysts for amidation of aldehydes with amines. *RSC Advances* **2015,** *5*, 94768-94775; (d) Cotton, S. A., Lanthanide Amides. In *Encyclopedia of Inorganic and Bioinorganic Chemistry*, John Wiley & Sons, Ltd: 2011; (e) Vitanova, D. V.; Hampel, F.; Hultzsch, K. C. Linked bis(β-diketiminato) yttrium and lanthanum complexes as catalysts in asymmetric hydroamination/cyclization of aminoalkenes (AHA). *J. Organomet. Chem.* **2011,** *696*, 321-330; (f) Döring, C.; Kempe, R. Synthesis and Structure of Aminopyridinato-Stabilized Yttrium and Lanthanum Amides and Their Reactivity towards Alkylaluminium Compounds. *Eur. J. Inorg. Chem.* **2009,** *2009*, 412-418; (g) Korobkov, I.; Gambarotta, S. Aluminate Samarium(II) and Samarium(III) Aryloxides. Isolation of a Single-Component Ethylene Polymerization Catalyst. *Organometallics* **2009,** *28*, 4009-4019; (h) Hong, S.; Tian, S.; Metz, M. V.; Marks, T. J. C2-Symmetric Bis(oxazolinato)lanthanide Catalysts for Enantioselective Intramolecular Hydroamination/Cyclization. *J. Am. Chem. Soc.* **2003,** *125*, 14768-14783; (i) Dash, A. K.; Razavi, A.; Mortreux, A.; Lehmann, C. W.; Carpentier, J.-F. Amine Elimination Reactions between Homoleptic Silylamide Lanthanide Complexes and an Isopropylidene-Bridged Cyclopentadiene−Fluorene System. *Organometallics* **2002,** *21*, 3238-3249; (j) Belot, J. A.; Wang, A.; McNeely, R. J.; Liable-Sands, L.; Rheingold, A. L.; Marks, T. J. Highly Volatile, Low Melting, Fluorine-Free Precursors for Metal-Organic Chemical Vapor Deposition of Lanthanide Oxide-

Containing Thin Films. *Chem. Vap. Deposition* **1999,** *5*, 65-69; (k) Tian, S.; Arredondo, V. M.; Stern, C. L.; Marks, T. J. Constrained Geometry Organolanthanide Catalysts. Synthesis, Structural Characterization, and Enhanced Aminoalkene Hydroamination/Cyclization Activity. *Organometallics* **1999,** *18*, 2568-2570.

13. (a) Roesky, P., *Molecular Catalysis of Rare-Earth Elements*. Springer-Verlag Berlin Heidelberg: 2010; Vol. 137; (b) Müller, T. E.; Hultzsch, K. C.; Yus, M.; Foubelo, F.; Tada, M. Hydroamination: Direct Addition of Amines to Alkenes and Alkynes. *Chem. Rev.* **2008,** *108*, 3795-3892; (c) Hong, S.; Marks, T. J. Organolanthanide-Catalyzed Hydroamination. *Acc. Chem. Res.* **2004,** *37*, 673-686; (d) Anwander, R., Lanthanide amides. In *Organolanthoid Chemistry: Synthesis, Structure, Catalysis*, Springer Berlin Heidelberg: Berlin, Heidelberg, 1996; pp 33-112; (e) Weiss, C. J.; Marks, T. J. Organo-f-element catalysts for efficient and highly selective hydroalkoxylation and hydrothiolation. *Dalton Trans.* **2010,** *39*, 6576-6588; (f) Seo, S.; Marks, T. J. Lanthanide-Catalyst-Mediated Tandem Double Intramolecular Hydroalkoxylation/Cyclization of Dialkynyl Dialcohols: Scope and Mechanism. *Chem. - Eur. J.* **2010,** *16*, 5148-5162; (g) Seo, S.; Yu, X.; Marks, T. J. Intramolecular Hydroalkoxylation/Cyclization of Alkynyl Alcohols Mediated by Lanthanide Catalysts. Scope and Reaction Mechanism. *J. Am. Chem. Soc.* **2009,** *131*, 263-276; (h) Yu, X.; Seo, S.; Marks, T. J. Effective, Selective Hydroalkoxylation/Cyclization of Alkynyl and Allenyl Alcohols Mediated by Lanthanide Catalysts. *J. Am. Chem. Soc.* **2007,** *129*, 7244-7245; (i) Horino, Y.; Livinghouse, T. Alkene and Diene Hydrosilylations Catalyzed by Lanthanum Tris[bis(trimethylsilyl)amide]†. *Organometallics* **2004,** *23*, 12-14; (j) Kawaoka, A. M.; Douglass, M. R.; Marks, T. J. Homoleptic Lanthanide Alkyl and Amide Precatalysts Efficiently Mediate Intramolecular Hydrophosphination/Cyclization. Observations on Scope and Mechanism. *Organometallics* **2003,** *22*, 4630-4632; (k) Horino, Y.; Livinghouse, T.; Stan, M. Alkene-

pinacolborane hydroborations catalyzed by lanthanum tris[bis(trimethylsilyl)amide]. *Synlett* **2004**, 2639-2641; (l) Hong, S.; Kawaoka, A. M.; Marks, T. J. Intramolecular Hydroamination/Cyclization of Conjugated Aminodienes Catalyzed by Organolanthanide Complexes. Scope, Diastereo- and Enantioselectivity, and Reaction Mechanism. *J. Am. Chem. Soc.* **2003,** *125*, 15878-15892; (m) Bürgstein, M. R.; Berberich, H.; Roesky, P. W. Homoleptic Lanthanide Amides as Homogeneous Catalysts for Alkyne Hydroamination and the Tishchenko Reaction. *Chem. Eur. J.* **2001,** *7*, 3078-3085.

14. (a) Agarwal, S.; Karl, M.; Dehnicke, K.; Seybert, G.; Massa, W.; Greiner, A. Ring-opening polymerization of ε-caprolactone and δ-valerolactone using new Sm(III) μ-halo-bis(trimethylsilyl)amido complexes. *J. Appl. Polym. Sci.* **1999,** *73*, 1669-1674; (b) Hultzsch, K. C.; Spaniol, T. P.; Okuda, J. Chiral Lanthanocene Derivatives Containing Two Linked Amido−Cyclopentadienyl Ligands: Heterobimetallic Structure and Lactone Polymerization Activity. *Organometallics* **1997,** *16*, 4845-4856.

15. (a) Crozier, A. R.; Törnroos, K. W.; Maichle-Mössmer, C.; Anwander, R. Trivalent cerium and praseodymium aromatic Ketone adducts. *Eur. J. Inorg. Chem.* **2013**, 409-414; (b) Allen, M.; Aspinall, H. C.; Moore, S. R.; Hursthouse, M. B.; Karvalov, A. I. Benzophenone complexes of the lanthanides: Synthesis of [Ln{N(SiMe$_3$)$_2$}$_3$(Ph2CO)] (L = La, Eu, Tb, Yb or Y) and X-ray crystal structure of the terbium complex. *Polyhedron* **1992,** *11*, 409-413.

16. Ohki, Y.; Takikawa, Y.; Hatanaka, T.; Tatsumi, K. Reductive N−N Bond Cleavage of Diphenylhydrazine and Azobenzene Induced by Coordinatively Unsaturated Cp*Fe{N(SiMe$_3$)$_2$}. *Organometallics* **2006,** *25*, 3111-3113.

17. Dudnik, A. S.; Weidner, V. L.; Motta, A.; Delferro, M.; Marks, T. J. Atom-efficient regioselective 1,2-dearomatization of functionalized pyridines by an earth-abundant organolanthanide catalyst. *Nat. Chem.* **2014,** *6*, 1100-1107.

18. (a) Bakewell, C.; White, A. J. P.; Long, N. J.; Williams, C. K. Metal-Size Influence in Iso-Selective Lactide Polymerization. *Angew. Chem. Int. Ed.* **2014,** *53*, 9226-9230; (b) Evans, W. J.; Sollberger, M. S.; Hanusa, T. P. Synthesis and structure of the polymetallic yttrium alkoxide complex $Y_3(\mu\text{-}OCMe_3)(\mu_3\text{-}Cl)(\mu\text{-}OCMe_3)_3(OCMe_3)_4(THF)_2$ and related complexes: $Ln_3(\mu_3\text{-}OR)(\mu_3\text{-}X)(\mu\text{-}OR)_3$ building blocks in yttrium and lanthanide alkoxide chemistry. *J. Am. Chem. Soc.* **1988,** *110*, 1841-1850.

19. (a) Horino, Y.; Livinghouse, T. Alkene and Diene Hydrosilylations Catalyzed by Lanthanum Tris[bis(trimethylsilyl)amide]. *Organometallics* **2004,** *23*, 12-14; (b) Fegler, W.; Venugopal, A.; Kramer, M.; Okuda, J. Molecular Rare-Earth-Metal Hydrides in Non-Cyclopentadienyl Environments. *Angew. Chem. Int. Ed.* **2015,** *54*, 1724-1736; (c) Nishiura, M.; Guo, F.; Hou, Z. Half-Sandwich Rare-Earth-Catalyzed Olefin Polymerization, Carbometalation, and Hydroarylation. *Acc. Chem. Res.* **2015,** *48*, 2209-2220; (d) Konkol, M.; Okuda, J. Non-metallocene hydride complexes of the rare-earth metals. *Coord. Chem. Rev.* **2008,** *252*, 1577-1591; (e) Harrison, K. N.; Marks, T. J. Organolanthanide-catalyzed hydroboration of olefins. *J. Am. Chem. Soc.* **1992,** *114*, 9220-9221; (f) Watson, P. L. Facile C-H activation by lutetium-methyl and lutetium-hydride complexes. *J. Chem. Soc., Chem. Commun.* **1983**, 276-277.

20. Laidler, K. J., *Chemical Kinetics*. Pearson Education: 1987.

21. Midland, M. M.; Zderic, S. A. Kinetics of reductions of substituted benzaldehydes with B-alkyl-9-borabicyclo[3.3.1]nonane (9-BBN). *J. Am. Chem. Soc.* **1982,** *104*, 525-528.

22. Kozuch, S.; Shaik, S. How to Conceptualize Catalytic Cycles? The Energetic Span Model. *Acc. Chem. Res.* **2011,** *44*, 101-110.

23. Jaffé, H. H. A Reëxamination of the Hammett Equation. *Chem. Rev.* **1953,** *53*, 191-261.

24. (a) Liu, H.; Khononov, M.; Eisen, M. S. Catalytic 1,2-Regioselective Dearomatization of N-Heteroaromatics via a Hydroboration. *ACS Catal.* **2018,** *8*, 3673-3677; (b) Zhang, F.; Song, H.; Zhuang, X.; Tung, C.-H.; Wang, W. Iron-Catalyzed 1,2-Selective Hydroboration of N-Heteroarenes. *J. Am. Chem. Soc.* **2017,** *139*, 17775-17778.

25. Chong, C. C.; Hirao, H.; Kinjo, R. Metal-Free σ-Bond Metathesis in 1,3,2-Diazaphospholene-Catalyzed Hydroboration of Carbonyl Compounds. *Angew. Chem., Int. Ed.* **2015,** *54*, 190-194.

26. Weetman, C.; Anker, M. D.; Arrowsmith, M.; Hill, M. S.; Kociok-Kohn, G.; Liptrot, D. J.; Mahon, M. F. Magnesium-catalysed nitrile hydroboration. *Chem. Sci.* **2016,** *7*, 628-641.

27. Hartwig, J. F.; Bhandari, S.; Rablen, P. R. Addition of Catecholborane to a Ruthenium-Alkyl: Evidence for .sigma.-Bond Metathesis with a Low-Valent, Late Transition Metal. *J. Am. Chem. Soc.* **1994,** *116*, 1839-1844.

28. Berberich, H.; Roesky, P. W. Homoleptic Lanthanide Amides as Homogeneous Catalysts for the Tishchenko Reaction. *Angew. Chem. Int. Ed.* **1998,** *37*, 1569-1571.

29. Tucker, C. E.; Davidson, J.; Knochel, P. Mild and stereoselective hydroborations of functionalized alkynes and alkenes using pinacolborane. *J. Org. Chem.* **1992,** *57*, 3482-3485.

30. (a) Yang, S. H.; Huh, J.; Jo, W. H. Density Functional Study on the Regioselectivity of Styrene Polymerization with an ansa-Metallocene Catalyst. *Organometallics* **2006,** *25*, 1144-1150;

(b) Yang, S. H.; Huh, J.; Yang, J. S.; Jo, W. H. A Density Functional Study on the Stereoselectivity of Styrene Polymerization with ansa-Metallocene Catalyst. *Macromolecules* **2004,** *37*, 5741-5751.

31. Rassolov, V. A.; Pople, J. A.; Ratner, M. A.; Windus, T. L. 6-31G* basis set for atoms K through Zn. *The Journal of Chemical Physics* **1998,** *109*, 1223-1229.

32. Yu, Y. B.; Privalov, P. L.; Hodges, R. S. Contribution of translational and rotational motions to molecular association in aqueous solution. *Biophys. J.* **2001,** *81*, 1632-1642.

33. Gaussian 16, R. B., Frisch, M.J. *et al*. Gaussian, Inc., Wallingford CT, **2016**.